



HAL
open science

Heterogeneous Influence of Glacier Morphology on the Mass Balance Variability in High Mountain Asia

F. Brun, P. Wagnon, E. Berthier, Vincent Jomelli, S. Maharjan, F. Shrestha, P. Kraaijenbrink

► **To cite this version:**

F. Brun, P. Wagnon, E. Berthier, Vincent Jomelli, S. Maharjan, et al.. Heterogeneous Influence of Glacier Morphology on the Mass Balance Variability in High Mountain Asia. *Journal of Geophysical Research: Earth Surface*, 2019, 124 (6), pp.1331-1345. 10.1029/2018JF004838 . hal-02989853v1

HAL Id: hal-02989853

<https://hal.science/hal-02989853v1>

Submitted on 4 Dec 2020 (v1), last revised 8 Apr 2021 (v2)

HAL is a multi-disciplinary open access archive for the deposit and dissemination of scientific research documents, whether they are published or not. The documents may come from teaching and research institutions in France or abroad, or from public or private research centers.

L'archive ouverte pluridisciplinaire **HAL**, est destinée au dépôt et à la diffusion de documents scientifiques de niveau recherche, publiés ou non, émanant des établissements d'enseignement et de recherche français ou étrangers, des laboratoires publics ou privés.

Heterogeneous influence of glacier morphology on the mass balance variability in High Mountain Asia

F. Brun^{1,2}, P. Wagnon¹, E. Berthier², V. Jomelli³, S.B. Maharjan⁴, F.
Shrestha⁴, and P.D.A. Kraaijenbrink⁵

¹Univ. Grenoble Alpes, CNRS, IRD, Grenoble INP, IGE, F-38000 Grenoble, France

²LEGOS, Université de Toulouse, CNES, CNRS, IRD, UPS, F-31400 Toulouse, France

³Université Paris 1 Panthéon-Sorbonne, CNRS Laboratoire de Géographie Physique, 92195 Meudon,

France

⁴International Center for Integrated Mountain Development (ICIMOD), Kathmandu, Nepal

⁵Department of Physical Geography, Faculty of Geosciences, Utrecht University, Utrecht, the Netherlands

Key Points:

- Debris-free and debris-covered glaciers have statistically indistinguishable glacier-wide mass balances over 2000-2016
- Lake-terminating glaciers have on average more negative mass balances than land-terminating glaciers
- Morphological variables explain 8 to 48 % of the variance of High Mountain Asia glacier mass balances for the period 2000-2016

This article has been accepted for publication and undergone full peer review but has not been through the copyediting, typesetting, pagination and proofreading process which may lead to differences between this version and the Version of Record. Please cite this article as doi: 10.1029/2018JF004838

Corresponding author: Fanny Brun, fanny.brun@univ-grenoble-alpes.fr

Abstract

We investigate the control of the morphological variables on the 2000-2016 glacier-wide mass balances of 6 470 individual glaciers of High Mountain Asia. We separate the dataset into 12 regions assumed to be climatically homogeneous. We find that the slope of the glacier tongue, mean glacier elevation, percentage of supra-glacial debris cover and avalanche contributing area all together explain a maximum of 48 % and a minimum of 8 % of the glacier-wide mass balance variability, within a given region. The best predictor of the glacier-wide mass balance is the slope of the glacier tongue and the mean glacier elevation for most regions, with the notable exception of the inner Tibetan Plateau. Glacier wide mass balances do not differ significantly between debris-free and debris-covered glaciers in seven of the twelve regions analysed. Lake-terminating glaciers have more negative mass balances than the regional averages, the influence of lakes being stronger on small glaciers than on large glaciers.

1 Introduction

Glacier mass balance is widely recognized as a sensitive indicator of climate change [e.g., *Bojinski et al.*, 2014]. Recent studies showed the contrasted glacier mass changes at the scale of the Pamir-Karakoram-Himalaya, and even at the scale of the entire High Mountain Asia (HMA) for the beginning of the twenty-first century [e.g., *Kääb et al.*, 2015; *Gardelle et al.*, 2013; *Gardner et al.*, 2013; *Brun et al.*, 2017]. Causes of these spatio-temporal changes are still not fully understood, because the climate variability is not well constrained, and because the response of each individual glacier to climate variability is modulated by its morphology, further complicating the interpretation of glacier mass changes. Heterogeneous climatology [*Maussion et al.*, 2014] could be responsible for various glacier mass balance sensitivities to temperature, explaining partly the regional pattern of recent glacier mass changes [*Sakai and Fujita*, 2017]. Other studies highlighted the role of heterogeneity of climate change itself, in explaining the regional pattern of glacier mass balance [e.g., *Kapnick et al.*, 2014; *Forsythe et al.*, 2017]. The morphology

46 of the glaciers and their catchments, and the abundance of supra-glacial debris show large
47 variations in HMA, and may also explain part of the variability of glacier mass balance.

48 Previous studies showed that, in the European Alps, annual fluctuations of glacier-
49 wide mass balance are strongly correlated in a given region [e.g., *Vincent et al.*, 2017],
50 and are related to meteorological annual fluctuations [e.g., *Rabatel et al.*, 2013]. Never-
51 theless, multi-decadal averages of individual glacier mass balances are linked to glacier
52 morphology [e.g., *Paul and Haeberli*, 2008; *Huss*, 2012; *Huss et al.*, 2012; *Rabatel et al.*,
53 2013; *Fischer et al.*, 2015; *Rabatel et al.*, 2016]. For instance, *Huss* [2012] found that a
54 combination of six morphological variables explained 51 % of the glacier mass balance
55 variance. For HMA, *Salerno et al.* [2017] conducted a statistical analysis of the thinning
56 rates of glaciers in the Everest region, in relationship with morphological variables. They
57 found that the slope of the glacier tongue was the main morphological variable control-
58 ling the glacier thickness changes, and they suggested that this was partially explained
59 by preferential development of glacial ponds on shallow slopes [e.g., *Quincey et al.*, 2007].
60 To our knowledge this is the only study investigating the link between glacier thickness
61 changes and morphological variables in HMA, and it is limited to a small region (360 km²
62 of ice).

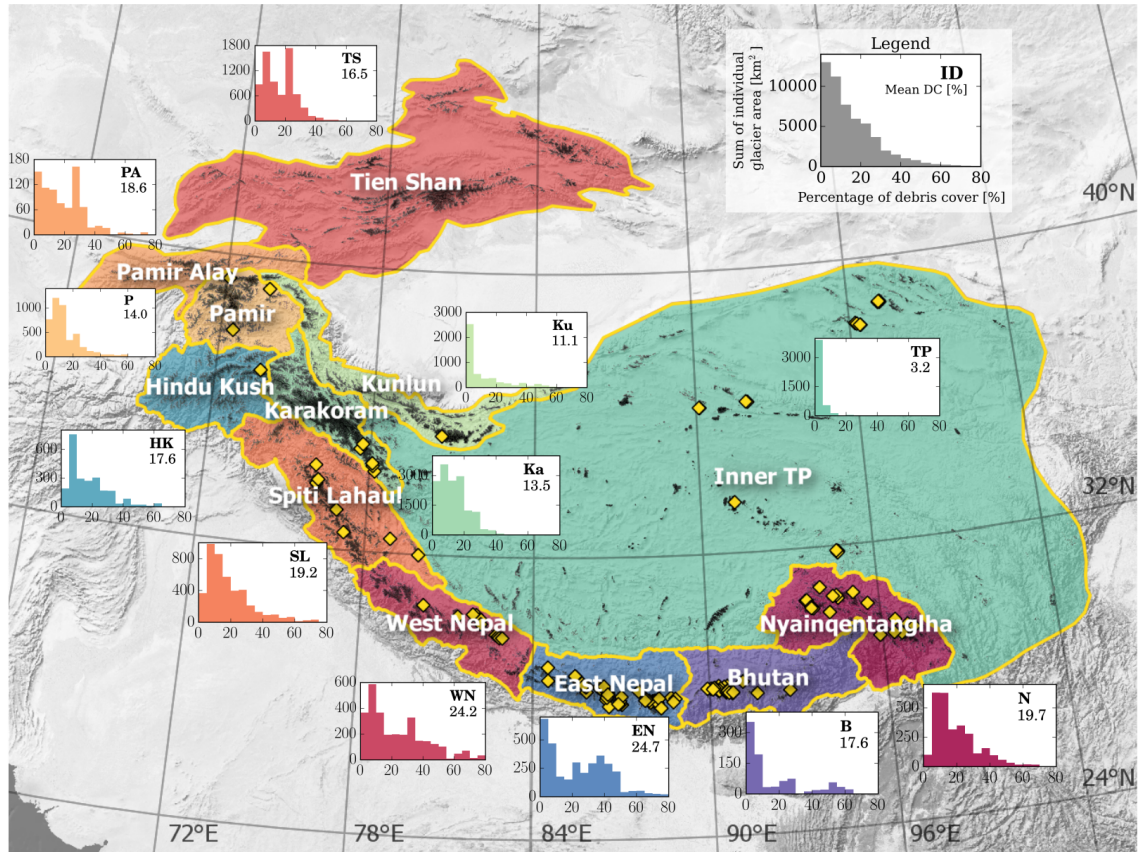
63 The influence of debris at the surface of many HMA glaciers is the subject of an
64 ongoing debate, and requires more investigation at large spatial scale. Geodetic stud-
65 ies suggested similar thinning rates over debris-free and debris-covered ice for ablation
66 tongues in the same elevation range [*Nuimura et al.*, 2012; *Gardelle et al.*, 2012, 2013;
67 *Kääb et al.*, 2012]. This finding is in apparent contradiction with the reduced ablation
68 expected for ice beneath a thick debris layer [e.g., *Nicholson and Benn*, 2006]. *Salerno*
69 *et al.* [2017] also investigated this question, and found that the presence of supra-glacial
70 debris cover was not a significant contributor to differences in thinning rates among the
71 studied glaciers. However, they examined a restricted sample of glaciers (n = 28) and
72 analyzed only tongue-averaged thinning rates, which are less straightforward to inter-

73 pret than glacier-wide mass balances as they result from the sum of surface mass bal-
74 ance and emergence velocity [e.g., *Cuffey and Paterson*, 2010]. Consequently, there is
75 a need to test this hypothesis over the glacier-wide mass balances of a larger number of
76 glaciers and in different climate contexts.

77 Furthermore, the development of pro-glacial lakes at glacier termini is a topic of
78 interest in HMA, as they are associated with enhanced glacier mass loss through sub-
79 aqueous melting [e.g., *Röhl*, 2006], accelerated ice flows [e.g., *King et al.*, 2018] and with
80 potential hazardous glacier lake outburst floods [GLOFs; e.g., *Haritashya et al.*, 2018].
81 Compared with land-terminating glaciers, lake-terminating glaciers shrink faster in Sikkim
82 [*Basnett et al.*, 2013], have more negative rates of elevation changes in Bhutan, Everest
83 region and West Nepal [*Gardelle et al.*, 2013] and have more negative mass balances in
84 the Everest region [*King et al.*, 2017]. Terminal lakes develop when supraglacial ponds
85 coalesce into a single lake dammed by a terminal moraine [e.g., *Benn et al.*, 2012; *Thomp-*
86 *son et al.*, 2012]. Eventually, the terminal lake enhances the frontal ablation by dynamic
87 thinning, calving and thermo-erosion [e.g., *Benn et al.*, 2012]. To our knowledge, the only
88 study quantifying the influence of terminal lake on glacier-wide mass balance was con-
89 ducted on 32 glaciers (9 of them being lake-terminating glaciers) and restricted to the
90 Everest region [*King et al.*, 2017].

91 In this study, we build upon the work of *Salerno et al.* [2017] and *King et al.* [2017].
92 We extend them by adding additional variables, such as the avalanche contributing area
93 and we extend the analysis to the entire HMA, by analyzing 6 470 individual glacier (>2
94 km²) mass changes in relationship with morphological variables. For each of the twelve
95 regions defined in *Brun et al.* [2017] and shown in Figure 1, i.e. Bhutan (B), East Nepal
96 (EN), Hindu Kush (HK), Inner Tibetan Plateau (TP), Karakoram (Ka), Kunlun (Ku),
97 Nyainqentanglha (N), Pamir (P), Pamir Alay (PA), Spiti Lahaul (SL), Tien Shan (TS)
98 and West Nepal (WN), we test whether supra-glacial debris cover reduces mass loss, whether
99 lake terminating glaciers have more negative mass balance and we assess the part of the

100 variance of glacier mass balance explained by the morphological variables. As we focus
 101 on debris-covered glaciers, we also extend the work of *Scherler et al.* [2011a], to assess
 102 the morphological specificities of debris-covered glaciers.

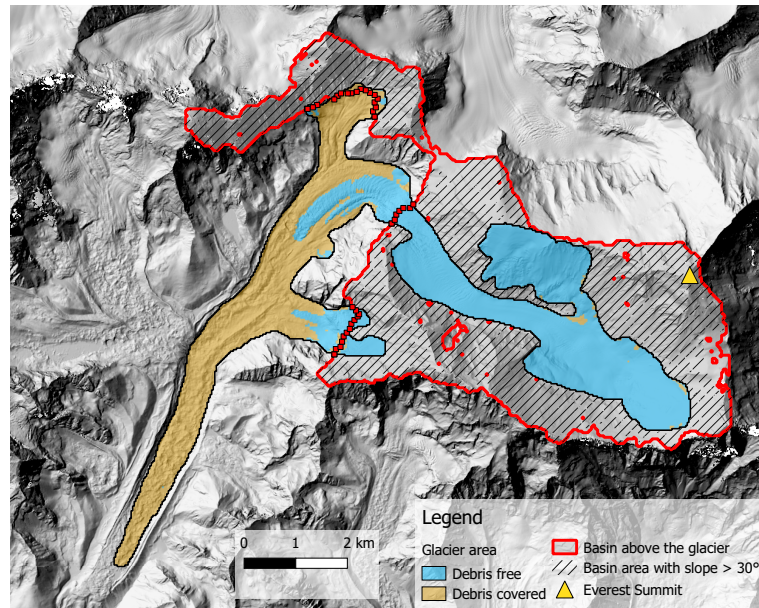


103 **Figure 1.** Distribution of the debris-covered and lake-terminating glaciers in HMA. The his-
 104 tograms represent the distributions of the supra-glacial debris cover percentage. The number is
 105 the percentage of the total glacierized area which is debris covered. The yellow diamonds repre-
 106 sent the locations of the lake-terminating glaciers studied here.

107 2 Data and methods

114 2.1 Glacier-wide mass balance and morphological data

115 The glacier-wide geodetic mass balance, \dot{M} (named glacier mass balance for sim-
 116 plicity hereafter) data are calculated from the rate of elevation change, extracted from

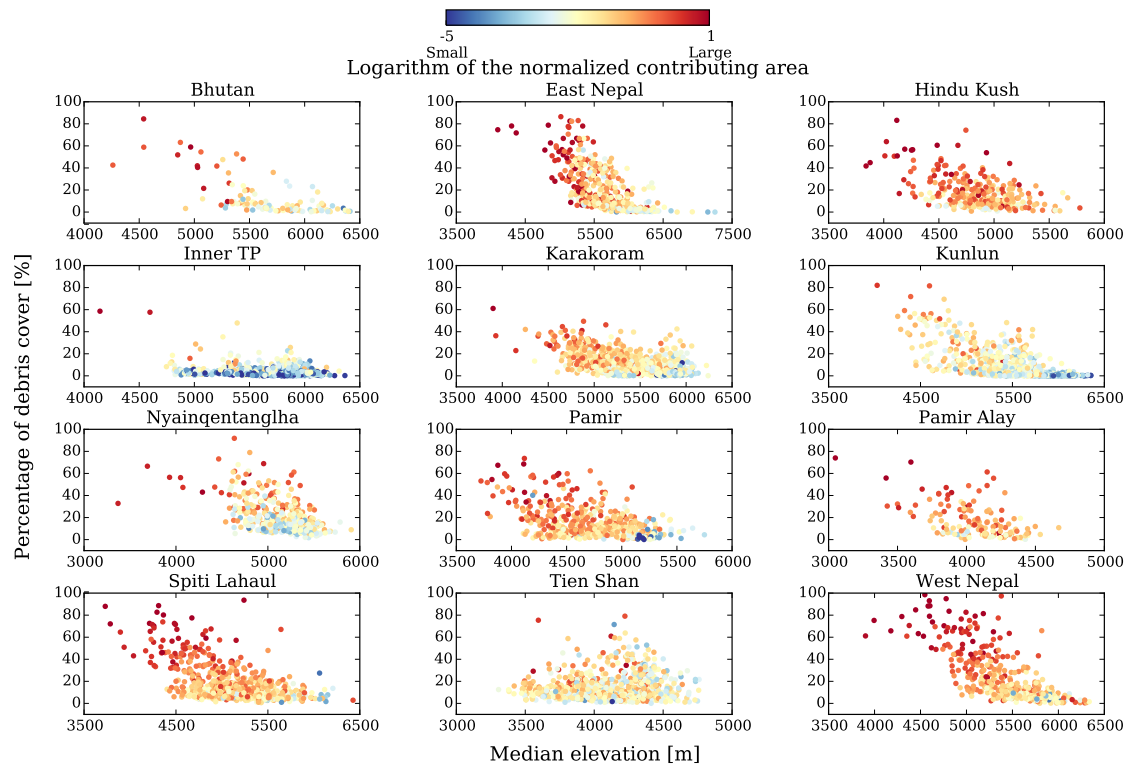


108 **Figure 2.** Example of the calculation of the avalanche contributing area for Khumbu Glacier
 109 (RGI ID 15.03733). The glacier area is classified either as debris-covered or debris-free follow-
 110 ing *Kraaijenbrink et al.* [2017], the basin above the glacier is the area (in grey) upstream of the
 111 glacier area above the glacier median elevation (red dashed line) and the avalanche accumulat-
 112 ing area is the parts of this basin where the slopes are steeper than 30° (hatched area). The
 113 background is a hillshade derived from the HMA DEM [*Shean, 2017*].

118 a linear fit of multi-temporal digital elevation models (DEMs) obtained from the Advanced
 119 Spaceborne Thermal Emission and Reflection Radiometer (ASTER), as described in *Brun*
 120 *et al.* [2017]. Only glaciers larger than 2 km^2 are included to limit the error on the glacier
 121 mass balance, which decreases with increasing glacier area [*Rolstad et al., 2009*]. Glaciers
 122 with less than 70 % of reliable elevation change rates are excluded from the analysis, lead-
 123 ing to a total number of 6 480 glaciers. Even though the majority of the $\sim 95\,000$ glaciers
 124 of HMA are excluded from this analysis due to their small size, our sample still repre-
 125 sents 54 % of the total glacierized area of the HMA [*Pfeffer et al., 2014*]. The glacier mass
 balances are calculated using the RGI 5.0 glacier mask [*Pfeffer et al., 2014*], which is based

126 mostly on satellite images acquired in the early 2000s. For a discussion about the influ-
127 ence of the uncertainties of the glacier inventory on the geodetic mass balance, the reader
128 is referred to the supplementary of *Brun et al.* [2017]. The individual glacier mass bal-
129 ances have a median uncertainty of ± 0.22 m w.e. a^{-1} , ranging from a minimum of \pm
130 0.14 to a maximum of ± 0.89 m w.e. a^{-1} [*Brun et al.*, 2017].

135 In this study we explore glacier morphological variables [area, aspect, mean slope,
136 slope of the lowest 20 % (tongue slope), mean elevation (mean elev.), median elevation,
137 minimum elevation, maximum elevation, area percentage of supra-glacial debris cover
138 (DC), and avalanche contributing area (contrib. area)] found to have an influence on
139 mass balance in previous studies [e.g., *Huss*, 2012; *Fischer et al.*, 2015; *Salerno et al.*,
140 2017]. The glacier morphological variables are calculated from the gridded debris cover
141 classification and elevation raster by *Kraaijenbrink et al.* [2017], which are clipped to the
142 RGI 5.0 glacier extents and have a resolution of 30 m. All the areas are calculated as
143 planar areas [*Cogley et al.*, 2011]. The glacier mean aspect (in degree) is calculated as
144 the vector average of the aspect of individual pixels in order to avoid the typical prob-
145 lems due to direct averaging of discontinuous aspect values. The mean slope (in degree)
146 is calculated as direct average of the slope of individual pixels, and the tongue slope as
147 the average of the slope of the pixels with an elevation below the 20th percentile of the
148 elevation for this glacier. The area percentage of supra-glacial debris cover is calculated
149 as the ratio of the glacier area classified as debris or as supra-glacial ponds divided by
150 the total glacier area. The avalanche contributing area (in km^2) is defined as the non-
151 glacierized area in the catchment upstream of the glacier median elevation with a slope
152 steeper than 30° (Figure 2). The catchment upstream of the median glacier elevation
153 is calculated based on the Shuttle Radar Topographic Mission (SRTM) 30 m void-filled
154 DEM [*Farr et al.*, 2007] and the upslope area module [*Freeman*, 1991] implemented in
155 the SAGA software [*Conrad et al.*, 2015]. More sophisticated approaches exist in the lit-
156 erature [e.g., *Bernhardt and Schulz*, 2010], but, even though the avalanche contributing
157 area significantly depends on the slope threshold, the correlation between this area and



31 **Figure 3.** Percentage of the glacier supra-glacial debris cover as a function of the glacier
 32 median elevation. The dots represent individual glaciers and are colored accordingly to the
 33 logarithm of their normalized avalanche contributing area, defined as the ratio of the avalanche
 34 contributing area divided by the glacier area.

158 the percentage of debris cover showed a very weak sensitivity to the slope threshold. Con-
159 sequently, we used a 30° threshold. Figure 2 illustrates these different areas for the ex-
160 ample of Khumbu Glacier (RGI Id 15.03733). Through the data analysis, we detected
161 some obvious outliers (10 glaciers), like for example glaciers with unrealistic low min-
162 imum elevation. These errors come from artifacts in the SRTM and we exclude these glaciers
163 from the analysis, leading to a final number of 6 470 glaciers.

166 2.2 Classification of debris-covered and debris-free glaciers

167 We propose to classify glaciers into two separate categories (debris-covered glaciers
168 and debris-free glaciers), based on the area percentage of supra-glacial debris cover. To
169 our knowledge there is no standard widely-accepted definition of what is a debris-covered
170 glacier. For instance, *Xiang et al.* [2018] use a 5 % threshold for the debris cover area
171 fraction, whereas *Janke et al.* [2015] use a 25 % threshold to define the debris-covered
172 glaciers. We determine an optimal threshold of 19 % of debris cover, based on 100 ran-
173 domly selected glaciers classified by five operators, as described in Supplementary Text
174 S1 [*Herreid and Pellicciotti*, 2018] and Supplementary Figures S1 and S2. It is notewor-
175 thy that this distinction is arbitrary, as there is a continuum between debris-covered and
176 debris-free glaciers. However we find useful to make this categorization, as it simplifies
177 the analysis. In our comparison between debris-covered and debris-free glaciers, we as-
178 sess the sensitivity of the glacier wide mass balances aggregated by glacier type to this
threshold by testing 14 % and 24 % thresholds.

180 2.3 Classification of lake-terminating and land-terminating glaciers

181 We automatically select the glaciers in contact with lakes (within a 50 m buffer)
182 from a lake inventory produced by the International Center for Integrated Mountain De-
183 velopment [*Maharjan et al.*, 2018] and the glacial lake inventory produced by *Zhang et al.*
184 [2017]. Both inventories are based on Landsat images collected in the early 2000s, with
185 a focus on the 2004-2007 period for the ICIMOD inventory. Then from visual inspec-

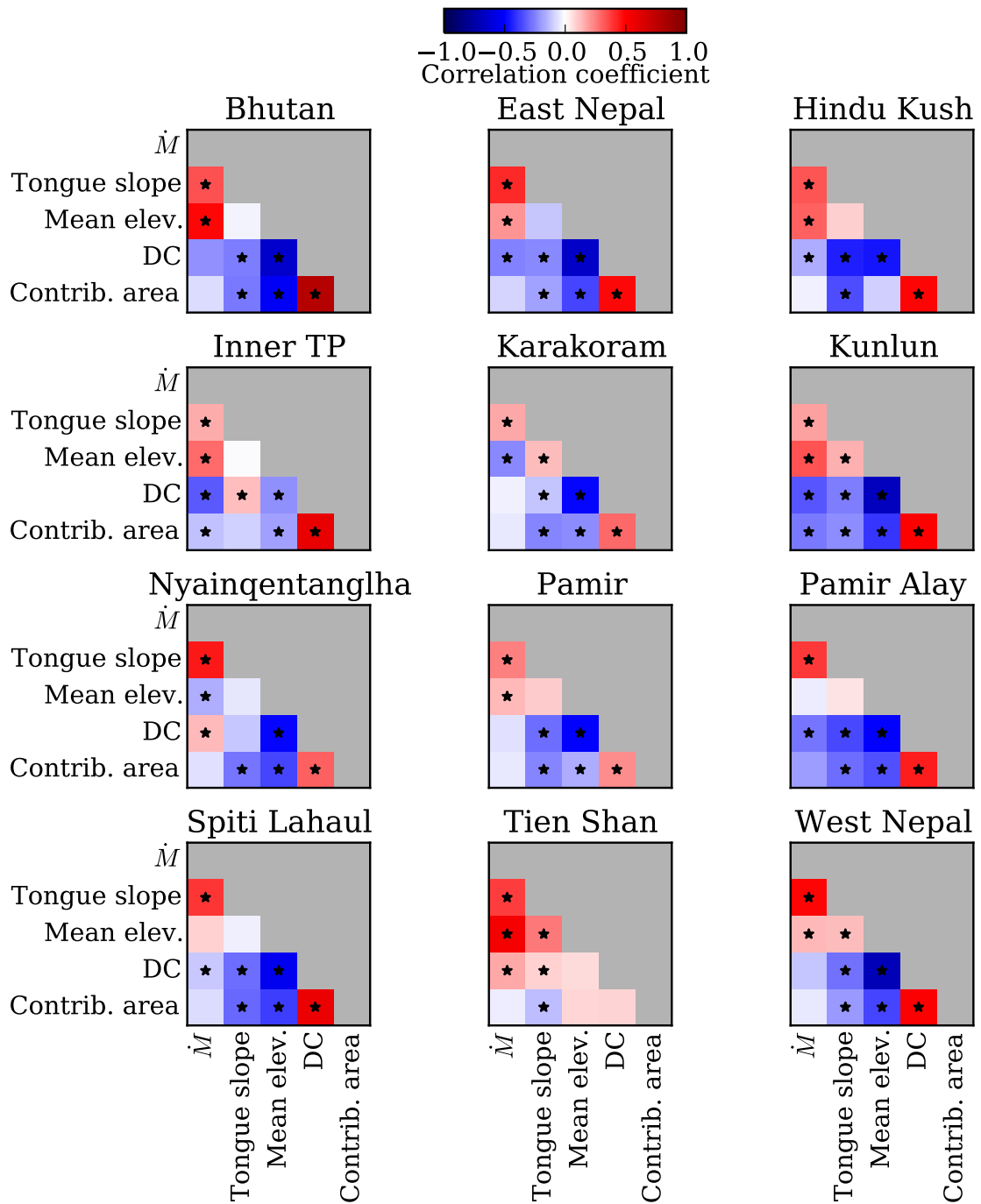


Figure 4. Pearson correlation coefficients between selected variables. The \star denotes correlation significant at $p < 0.01$.

186 tion of satellite images accessed through Google Earth , we retain 133 glaciers, which are
 187 actually lake-terminating glaciers. The lake inventory does not cover the Tien Shan and
 188 Pamir Alay regions and our samples include only 1, 1, 3 and 5 lake-terminating glaciers
 189 in Kunlun, Hindu Kush, Pamir and Karakoram, respectively. Consequently, we focus the
 190 analysis on the six remaining regions: Bhutan (21 lakes), East Nepal (47 lakes), inner
 191 Tibetan Plateau (16 lakes), Spiti Lahaul (7 lakes), West Nepal (11 lakes) and Nyainqen-
 192 tanglha (19 lakes). Eight of these glaciers are excluded from the analysis because we could
 193 not calculate their mass balance from ASTER DEMs (because they have less than 70
 194 % of reliable rate of elevation change coverage).

195 **2.4 Linear analysis and multivariate linear model**

196 We perform univariate linear analysis, by calculating the Pearson's correlation co-
 197 efficients and associated p -values for all the 2-by-2 combinations of available variables
 198 as well as, for some of them, their exponential and logarithmic values (Tables S1-12). We
 199 also implemented a simple multivariate linear model to determine the best predictors (and
 200 combination of predictors) of the glacier mass balance (\dot{M}) variability. This model aims
 201 at finding the set of coefficients ($\alpha_1, \alpha_2, \dots, \alpha_n$), which explains a maximum of the mass
 202 balance variance, when multiplying the predictors (x_1, x_2, \dots, x_n), such as:

$$\dot{M} = \alpha_1 x_1 + \alpha_2 x_2 + \dots + \alpha_n x_n \quad (1)$$

203 We worked with standardized predictors and standardized \dot{M} to allow for a direct com-
 204 parison between the coefficients α_i . The standardized predictor $x_{i,s}$ derived from the vari-
 205 able x_i is defined as:

$$x_{i,s} = \frac{x_i - \bar{x}_i}{\sqrt{V(x_i)}} \quad (2)$$

206 where \bar{x}_i is the variable regional average and $V(x_i)$ is its regional variance.

207 We explore the morphological variables that explain the maximum of the variance,
 208 but the selection of the different variables to include in the multivariate linear model is
 209 subjective and we could not find an optimal combination of variables which minimized

210 the Akaike Information Criterion [The AIC is a metric that penalizes models with a large
211 number of parameters; *Akaike*, 1974], while maximizing the explained variance (R^2) of
212 \dot{M} for all the regions simultaneously. Similarly, standard approaches such as the forward
213 selection and backward elimination, which consist in an evaluation of the model after
214 adding or removing variables until an optimal combination is reached, [e.g., *Hocking*, 1976],
215 give different results for different regions, mainly because some variables were very re-
216 dundant (for example the mean and the median elevation). These attempts to select the
217 best performing model in an objective way were not successful. Instead, we favor vari-
218 ables that are often selected in the literature, such as the supra-glacial debris cover or
219 the avalanche contributing area [*Huss et al.*, 2012; *Salerno et al.*, 2017]. We subjectively
220 choose the final variables and retain the tongue slope, the mean elevation, the area per-
221 centage of supra-glacial debris cover and the avalanche contributing area.

222 3 Results

223 3.1 Contrasted glacier morphologies in the different regions

224 Our analysis shows that the different regions have varying supra-glacial debris cover,
225 with mean percentage of supra-glacial debris cover ranging from 3.2 % in the inner TP
226 to 24.7 % in the East Nepal (Figure 1). With a threshold of 19 % to distinguish between
227 debris-free and debris-covered glaciers, we find that debris-covered glaciers occupy be-
228 tween 1.5 % of the total glacierized area in the inner TP and 56.7 % in the East Nepal
229 (Figure 1). The extent of supra-glacial debris cover is controlled by the local relief, and
230 in particular the area occupied by ice-free terrain above the glacier, which contributes
231 to the debris supply [*Scherler et al.*, 2011a]. We extend the analysis of *Scherler et al.* [2011a],
232 that cover only a limited number of glaciers (287) over selected regions (Hindu Kush,
233 Karakoram, Kunlun, Spiti Lahaul, West Nepal, East Nepal, Bhutan), to our sample of
234 6 47 glaciers and we search for the morphological variables that could explain part of the
235 variability of the supra-glacial debris cover. In all regions except Tien Shan, the percent-

age of supra-glacial debris cover increases with the avalanche contributing area, with a positive correlation with R ranging from 0.23 to 0.77 and $p < 0.001$ (Figure 4 and Tables S1-12). It decreases with increasing median elevation, with a negative correlation with R ranging from -0.69 to -0.22 and $p < 0.001$ (Figure 4 and Tables S1-12). Indeed, the insulating effect of debris allows for the existence of debris-covered tongues at low elevation (Figure 3). Very few glaciers are debris covered in the inner TP, where glaciers are often small ice caps (i.e. with no head-walls above their accumulation area). Glaciers located in Tien Shan do not follow the same distribution as in the other regions, as the supra-glacial debris cover is neither related with the median elevation, nor with the avalanche contributing area (Figure 3). With the exception of Inner TP and Tien Shan, we also found a significant negative correlation between the percentage of supra-glacial debris cover and the tongue slope, with R reaching a minimum of -0.44 and various levels of significance (Figure 4 and Tables S1-12). Other variables, such as glacier area or mean aspect, do not show systematic correlations with the percentage of supra-glacial debris cover and exhibit large region to region differences (Tables S1-12).

The lake-terminating glaciers are mostly located in the south-eastern margin of the HMA (Figure 1). The sample size is not large enough to perform a robust statistical analysis.

3.2 Influence of the supra-glacial debris cover on the mass balance variability

In this section, we test the influence of the percentage of supra-glacial debris cover on the mass balance variability in two ways: first we test the correlation between the percentage of supra-glacial debris cover and the mass balance and second, we test the difference between two populations of glaciers (debris-free versus debris-covered) in terms of region-wide mass balances.

First, we tested whether the supra-glacial debris cover reduces the glacier mass losses. This hypothesis is rejected as a positive and significant correlation between \dot{M} and DC

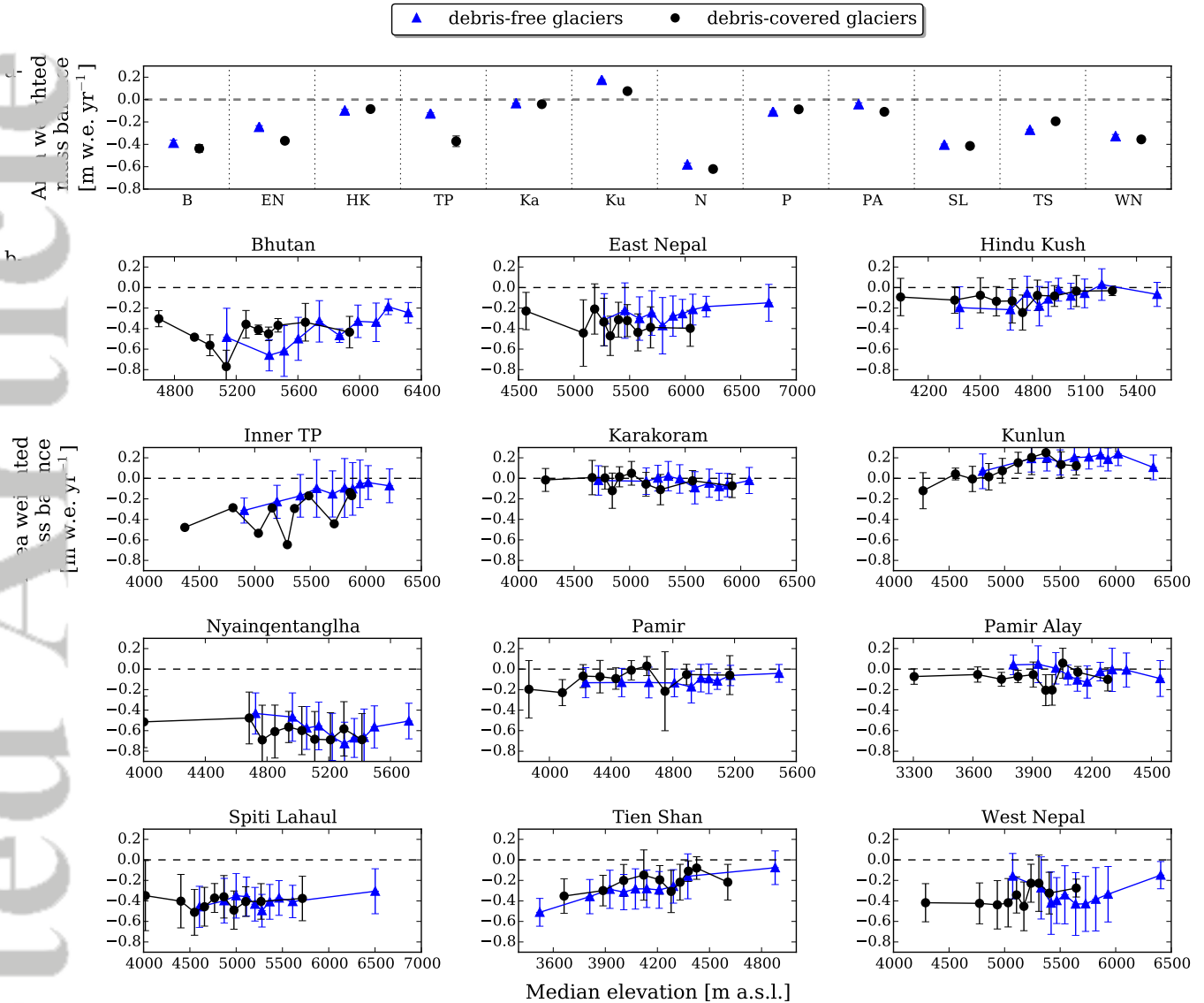


Figure 5. Glacier mass balances for debris-covered and debris-free glaciers; a- regional averages, and b- glaciers grouped by 10-percentiles of glacier mean elevation. The error bars represent the standard error on the mean, note that for the regional averages the dot size is most of the time larger than the error bars. The standard errors are smaller than the regional uncertainties of the glacier mass balance from *Brun et al.* [2017], because the latter takes into account the spatial correlation, whereas the standard error is used here to quantify the dispersion of the glacier population.

is found only for Tien Shan and Nyainqentanglha (Figure 4 and Tables S1-12). For all the other regions, the correlation was either negative or not significant.

Second, in terms of regional area weighted averages, debris-covered glaciers have a \dot{M} significantly (i.e., with a 95 % confidence *t*-test) more negative than debris-free glaciers in East Nepal, inner TP, Kunlun and Pamir Alay, with an absolute value of the difference ranging from 0.06 to 0.24 m w.e. a⁻¹ (Figure 5-a and Table 1). The later value corresponds to the inner TP, where we find only 11 debris-covered glaciers and consequently should be interpreted with caution. In Tien Shan it is the opposite (with the absolute value of the difference being 0.08 m w.e. a⁻¹), and for the remaining regions (seven in total) the differences are not significant.

When we group glaciers by mean elevations to calculate an averaged \dot{M} for each 10-percentile of mean elevation (Figure 5-b), slight statistically non-significant differences are apparent between regions. For instance, in East Nepal, Nyainqentanglha, Pamir Alay and in inner TP, the debris-covered glaciers have more negative \dot{M} at the same elevation, whereas it is the opposite for Bhutan, Pamir and Tien Shan.

These results are not very sensitive to the threshold used to discriminate between debris-free and debris-covered glaciers. Although the altitudinal distribution of debris-covered and debris-free glaciers is strongly modified if we use a threshold of 14 or 24 % to discriminate debris-covered and debris-free glaciers (Figures S3 and S4), the differences of \dot{M} between debris-free and debris-covered glaciers are close to the 19 % threshold differences (less than ± 0.05 m w.e. a⁻¹).

3.3 Influence of proglacial lakes on the mass balance variability

In general, lake-terminating glaciers have more negative \dot{M} than the regional average (Figure 6 and Table S13). They regularly lie further than one standard deviation from the mean. They have mean \dot{M} that are between 0.11 to 0.32 m w.e. a⁻¹ more negative than the regional averages, in Nyainqentanglha and West Nepal, respectively (Table S13). If we consider the relative differences, they have mean \dot{M} that are between 18

291 **Table 1.** Mean of the regional mass balance for debris-free (\dot{M}_{DF}) and debris-covered (\dot{M}_{DC})
 292 glaciers for each region in m w.e. a⁻¹. The standard error is calculated as the standard devia-
 93 tion of \dot{M} in m w.e. a⁻¹ divided by the square root of the number of glaciers in each sub-group
 94 (N_{DF} and N_{DC}). Note that the standard errors are smaller than the regional uncertainties of
 295 the glacier mass balance from *Brun et al.* [2017], because the latter takes into account the spa-
 296 tial correlation, whereas the standard error is used here to quantify the dispersion of the glacier
 97 population.

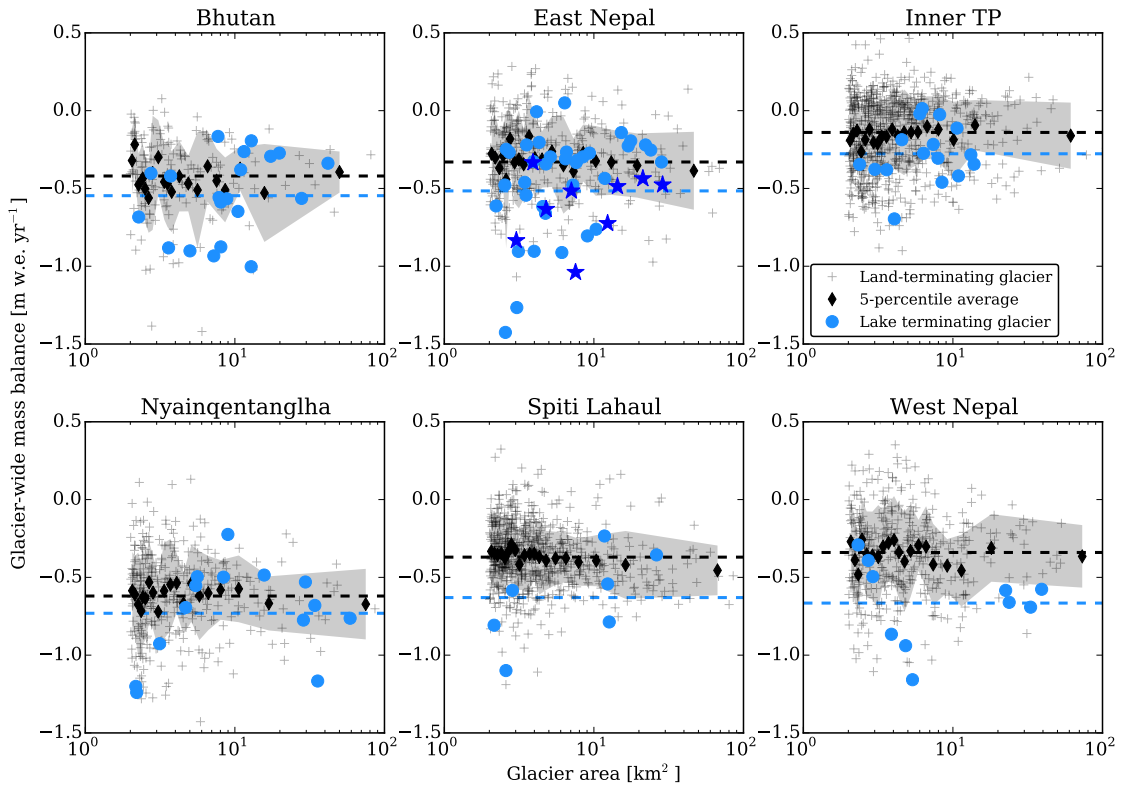
Region	B	EN	HK	TP	Ka	Ku	N	P	PA	SL	TS	WN
\dot{M}_{DF}	-0.39	-0.25	-0.10	-0.13	-0.04	0.17	-0.58	-0.11	-0.04	-0.41	-0.27	-0.33
Err. std. \dot{M}_{DF}	0.03	0.01	0.01	0.01	0.00	0.01	0.02	0.01	0.02	0.01	0.01	0.02
\dot{M}_{DC}	-0.44	-0.37	-0.08	-0.37	-0.04	0.08	-0.62	-0.09	-0.11	-0.41	-0.19	-0.36
Err. std. \dot{M}_{DC}	0.04	0.02	0.02	0.05	0.01	0.01	0.02	0.02	0.02	0.02	0.02	0.02
N_{DF}	80	271	196	719	1039	565	230	419	94	501	701	243
N_{DC}	24	161	100	11	138	120	161	132	47	179	175	173

304 to 98 % more negative than the regional averages, in Nyainqentanglha and inner TP, re-
305 spectively (Table S13). It is noteworthy that, the lake influence on \dot{M} decreases with the
306 glacier area, as the large lake-terminating glaciers tend to have \dot{M} closer to the regional
307 average than the small lake-terminating glaciers (Figure 6). The differences between \dot{M}
308 observed for lake terminating glaciers and \dot{M} predicted with the multivariate linear model
309 based on a combination of four variables (see below and Table S13) are mostly negative
310 (range: -0.44 to 0.07 m w.e. a⁻¹), meaning that the excess mass loss is likely to be at-
311 tributed to the presence of a lake at the glacier terminus and not to the glacier morphol-
312 ogy (i.e. the fact that they often exhibit a gently sloped tongue at the terminus for in-
313 stance).

321 3.4 Morphological variables and glacier mass balance variability

322 For selected regions, the morphological variables have various influences on \dot{M} and
323 different correlations among each others (Figure 4). Note that we do not present the re-
324 sults for all the variables described in the method section. The aspect and area are not
325 significant contributors to \dot{M} for almost all of the regions (Tables S1-12). The median
326 elevation, minimum elevation and maximum elevations are discarded because the mean
327 elevation is a better predictor in most cases, and is less sensitive to the quality of the in-
328 put DEM than the maximum and minimum elevations.

329 First, we investigate which variables have a high correlation with \dot{M} . \dot{M} has always
330 a significant positive correlation (R ranging from 0.16 to 0.49 with $p < 0.001$) with the
331 tongue slope (Figure 4), meaning the gentler the glacier slope, the more negative \dot{M} . Ex-
332 cept for Spiti Lahaul and Pamir Alai, the mean elevation is significantly correlated with
333 \dot{M} . This correlation is generally positive, with R ranging from 0.13 to 0.53 ($p < 0.01$
334 or $p < 0.001$), meaning the higher the glacier, the less negative \dot{M} . This correlation is
335 negative for Karakoram and Nyainqentanglha. For five regions (East Nepal, Hindu Kush,
336 Inner TP, Kunlun, Pamir Alay), the DC is significantly and negatively correlated with
337 \dot{M} , meaning the higher the debris cover, the more negative the glacier mass balance. How-



314 **Figure 6.** Glacier-wide mass balance as a function of glacier area. The black crosses represent
 315 the land terminating glaciers and the large blue dots the lake-terminating glaciers. The blue stars
 316 in East Nepal represent the nine lake-terminating glaciers studied by *King et al.* [2017]. The
 317 black diamonds represent the 5-percentile averages of all glaciers. The grey envelope represents
 318 the \pm one standard deviation from the mean. Note that for East Nepal, one lake-terminating
 319 glacier (with a size of 2.6 km^2) has a mass balance of $-1.9 \text{ m w.e. yr}^{-1}$ and therefore is missing
 320 on the plot.

338 ever, for the other regions, either it is the opposite (for Nyainqentanglha and Tien Shan),
339 or the correlation is not significant. The avalanche contributing area is usually not sig-
340 nificantly correlated with \dot{M} , except in Kunlun and inner TP where it is negatively cor-
341 related with \dot{M} (Tables S1-12).

342 Second, we calculated a multivariate linear model, which explains 8 to 48 % of \dot{M}
343 variability, based on a linear combination of four variables ignoring interaction between
344 the variables (Table 2). The regions where the explained variability is the lowest are the
345 Pamir, Karakoram and Kunlun. The regions where the explained variability is the high-
346 est are the Bhutan and Tien Shan. Except for the Kunlun region, the tongue slope is
347 always a significant predictor of \dot{M} variability and for seven regions out of twelve, it is
348 the predictor which has the largest α_i , and consequently, the strongest influence on \dot{M}
349 variability. The mean elevation has a significant contribution to \dot{M} variability for ten
350 regions out of twelve and has the largest α_i for four regions. The supra-glacial debris cover
351 has a significant contribution to \dot{M} variability for four regions and is sometimes posi-
352 tive and sometimes negative. It has the largest α_i only for the inner TP, with a nega-
353 tive value. Again this result is to be interpreted carefully, as the inner TP glaciers have
354 only 3.2 % of supra-glacial debris cover on average. In the other regions, it has a small
355 α_i compared with the other predictors. The avalanche contributing area is a significant
356 contributor to \dot{M} variability only for two regions. It has a small α_i (always less than half
357 of the largest α_i in absolute value) compared with the other predictors (Table 2).

365 4 Discussion

366 4.1 Limitations of our analysis

367 The statistical analysis presented here is sensitive to outliers, biases and uncertain-
368 ties in the data. The individual mass balance data have themselves a relatively high level
369 of uncertainty with a median uncertainty of 0.22 m w.e. a⁻¹ (ranging from 0.14 to 0.89
370 m w.e. a⁻¹), depending on the glacier area, on the proportion of the glacier surface sur-

Table 2. Results of the multivariate linear regression to explain the glacier mass balance variability for each region. The variables are standardized, and therefore the coefficients associated with each variable are directly representative of their relative influence on the glacier mass balance variability. R^2 is the squared Pearson coefficient for the multivariate linear regression, including all the predictors. We reported the coefficients (α_i), colored according to the p -values. The acronyms are the same one as used in Figure 1 and n is the number of glaciers considered in this study for each region.

Region	B	EN	HK	TP	Ka	Ku	N	P	PA	SL	TS	WN
Term. slope [-]	0.47	0.47	0.38	0.23	0.18	0.10	0.46	0.26	0.29	0.45	0.24	0.51
Mean elev. [-]	0.75	0.30	0.34	0.23	-0.34	0.21	-0.06	0.16	-0.19	0.17	0.47	0.18
DC [-]	0.09	0.00	0.13	-0.40	-0.16	-0.11	0.15	0.09	-0.23	0.06	0.12	0.12
Contrib. area [-]	0.37	0.11	0.07	0.17	-0.02	-0.10	-0.01	0.02	-0.07	0.09	-0.05	0.06
R^2	0.48	0.25	0.21	0.21	0.11	0.15	0.24	0.08	0.20	0.18	0.36	0.25
n	104	428	297	721	1176	684	391	552	141	679	877	416

$p < 0.001$	$p < 0.01$	$p < 0.1$	$p \geq 0.1$
-------------	------------	-----------	--------------

veyed and on the number of DEMs available to extract a reliable rate of elevation change
signal [Brun *et al.*, 2017]. The median uncertainty is slightly higher than the root mean
square error of 0.17 m w.e. a⁻¹ found when comparing ASTER \dot{M} with higher resolution
geodetic mass balances for 60 glaciers [Brun *et al.*, 2017]. In order to test the sen-
sitivity of two important results to this uncertainty, we perform a Monte Carlo test. We
randomly generate 1000 new series of \dot{M} . For each glacier, we randomly perturb the value
of \dot{M} following a normal distribution centered on the original value, with a standard de-
viation equals to the uncertainty on \dot{M} . We then repeat the same analysis as described
above to assess the robustness of the differences between the regional mean of debris-
covered and debris-free glaciers (Table S14), and to assess the robustness of the percent-
age of variance explained by the multivariate linear model (Figure S5). Regarding the
regional differences between debris-free and debris-covered glaciers, the results are very
robust, as a large majority (expressed in %) of perturbed simulations leads to the same
conclusion in terms of sign and significance of the difference (Table S14). Regarding the
robustness of the percentage of the variance explained by the linear model, the results
are less convincing, as the perturbed series systematically lead to lower R^2 (about ~ 0.1
lower on average), in particular for the Tien Shan and Nyainqentanglha (Figure S5).

The other data sources are also subject to uncertainty in the glacier delineation [Paul
et al., 2013], which, in turn, introduces large uncertainties in the debris cover extent, as
formerly glacierized areas, now free of glaciers, would be classified as debris-covered area.
The overall accuracy of the glacier surface classification is 91 % [Kraaijenbrink *et al.*, 2017].
Moreover, the avalanche contributing area is sensitive to the quality of the DEM used
to determine the upstream area of each glaciers [Tribe, 1992]. These intrinsic limitations
should be kept in mind.

One of the major limitation of our work is the use of non-independent variables as
explanatory variables in the multiple linear regression model. The tongue slope and mean
elevation are the best predictors of the mass balance variability. However, these variables
correlate with each other, and with the percentage of supra-glacial debris cover and avalanche

399 contributing area (Figure 4). This means that the influence of such correlated secondary
400 predictors cannot be interpreted within the multiple linear regression model framework,
401 and the univariate analysis (Tables S1-12) is more relevant in these cases. An alterna-
402 tive would be to introduce interaction terms (defined as $\alpha_{i,j}x_ix_j$ in our framework) in
403 the multiple linear model. More sophisticated approaches, such as a hierarchical Bayesian
404 approach could also help mitigate this issue, even though these approaches fail as well
405 when the level of correlation among explanatory variables exceeds ~ 0.6 [e.g., *Jomelli et al.*,
406 2015].

407 The separation of the glaciers into two distinct categories (debris-covered and debris-
408 free glaciers) is somehow arbitrary, as there is a continuum between these categories. Nev-
409 ertheless, the choice of different thresholds has a limited influence on the results (Fig-
410 ures 5, S3 and S4), and therefore the classification is still insightful.

411 Another limitation of our study is the separation of glaciers into regions that we
412 assumed climatically homogeneous. The regions considered in this study have a much
413 larger spatial extent than the Swiss or French Alps (< 300 and 200 km long, respectively),
414 as they spread from ~ 300 km (Pamir) to more than $2\,000$ km (inner TP). Regional di-
415 visions remain arbitrary and alternative delineations could be provided, based on climate
416 data clustering for example. This is especially true for regions such as the Tibetan Plateau
417 and the Tien Shan, where we group glaciers that are under very different climate influ-
418 ences [e.g., *Sakai and Fujita*, 2017].

19 **4.2 Specificities of debris-covered glaciers in terms of morphology and** 20 **mass balance variability**

421 Our results show that debris-covered tongues can be generally characterized as flat-
422 ter and located at lower elevations than debris-free tongues. Moreover, the avalanche con-
423 tributing area correlates strongly with the percentage of debris cover, hinting that large
424 part of the debris supply originates from the glacier upper reaches [e.g., *Wirbel et al.*,
425 2018]. These conclusions are in line with those of *Scherler et al.* [2011a], even though,

426 contrary to them, we do not include ice surface velocity in our analysis. The availabil-
427 ity of ice surface velocities for the entire ablation areas of HMA glaciers [*Dehecq et al.*,
428 2019] will help to further test the hypothesis of *Scherler et al.* [2011a], who observed sym-
429 metrical distributions of surface velocity for the debris-free glaciers and asymmetrical
430 distributions of surface velocity for the debris-covered glaciers.

431 We did not systematically observe less negative glacier-wide mass balances for debris-
432 covered glaciers, compared with debris-free glaciers. At the same time, *Nuimura et al.*
433 [2012], *Gardelle et al.* [2012, 2013] and *Kääb et al.* [2012] observed similar thinning rates
434 for debris-free and debris-covered tongues, which is not inconsistent with our observa-
435 tions given that thinning rates are a result not only on point mass balance but also on
436 emergence/submergence velocity [*Brun et al.*, 2018].

437 Even though we did not document glacier terminus changes, it was already shown
438 for selected regions of HMA that the debris-covered tongues experience less or no retreat
439 compared with debris-free tongues [e.g., *Scherler et al.*, 2011b; *Xiang et al.*, 2018]. How-
440 ever, debris-covered and debris-free glaciers have mostly similar \dot{M} , meaning that they
441 have to respond through different mechanisms to climate changes. The debris-covered
442 glaciers thin differently from the debris-free glaciers: debris-covered glacier thinning is
443 distributed over their lower reaches independently of the elevation, whereas debris-free
444 glaciers preferentially experience front retreat [*Rowan et al.*, 2015; *Rowan*, 2017; *Salerno*
445 *et al.*, 2017]. Consequently, the ice dynamics play a major role for the evolution of debris-
446 covered tongues, and the stable front positions of debris-covered glaciers should not be
447 interpreted as balance mass budget [*Scherler et al.*, 2011b].

448 4.3 Proglacial lake influence on glacier mass balance

449 In this study, we find that lake-terminating glaciers have \dot{M} 18 to 98 % more neg-
450 ative than the regional average. However, the lake influence depends on the glacier size
451 and the lake's stage of development [*Benn et al.*, 2012; *King et al.*, 2017]. Our more com-
452 plete mass balance dataset offers an opportunity to test the representativeness of the smaller

453 glacier sample used in *King et al.* [2017]. The glacier sample of *King et al.* [2017] has a
454 mean \dot{M} of -0.61 ± 0.11 m w.e. a^{-1} (versus -0.70 ± 0.27 m w.e. a^{-1} in their study), which
455 is slightly more negative than the average of all lake-terminating glaciers of East Nepal
456 (Figure 6). The results presented in this study are a broad regional overview, and more
457 studies should be conducted on specific lake-terminating glaciers to better understand
458 the lake influence on the glacier dynamics and mass balance [*King et al.*, 2018]. Local
459 studies are even more pressing because of the associated risk of GLOFs [*Haritashya et al.*,
460 2018]. In our study, we observe that there is no relationship between glacier-wide mass
461 balances of lake-terminating glaciers and the degree of danger of the associated lakes.

462 **4.4 Complex influence of the morphological variables on the glacier mass** 463 **balance**

464 The morphological variables explain 8 to 48 % of \dot{M} variance, with contrasted re-
465 gional behaviors. Qualitatively, it seems that the regions where \dot{M} is the most negative
466 (Nyainqentanglha, Bhutan, Tien Shan) are the regions where the morphological variables
467 explain the largest part of the variance. Our interpretation of this observation remains
468 rather speculative. A possibility is that morphological variables are linked to glacier re-
469 sponse time and glacier mass balance sensitivity to climate change. Indeed, response times
470 of glaciers with low slopes at their terminus, and in turn with slow dynamics, are longer
471 than steep glaciers. Consequently, their geometry does not adapt quickly to changes in
472 climate, they remain in imbalance for a longer time, and their mass balance is driven to-
473 ward negative values explaining why the correlation between \dot{M} and morphological vari-
474 ables such as the slope is high [*Cuffey and Paterson*, 2010]. Similarly, glaciers lying at
475 low elevations are expected to receive more precipitation and to have a larger accumu-
476 lation basin than glaciers at high elevations, in order to balance higher ablation in the
477 lower reaches. These glaciers have a larger mass turnover, and consequently they are more
478 sensitive to an increase in temperature [*Oerlemans and Reichert*, 2000].

479 Studies focusing in the Alps found comparable influences of morphological variables
480 on \dot{M} variability, although this region is climatically and topographically different from
31 the regions of our study. In the Swiss Alps, *Huss* [2012] found that a combination of 3
482 variables (area, median glacier elevation and slope of the tongue) explained 35 % of the
483 variance of a sample of 50 glacier mass balances averaged over 100 years. The explained
484 variance reached 51 % when using a combination of 6 variables (the former three vari-
35 ables, the latitude, the longitude and the aspect). In the French Alps, *Rabatel et al.* [2016]
36 found that the slope of the tongue and the glacier median elevation explained 25 % of
487 the variance of a sample of 30 glacier mass balances averaged over 31 years. The anti-
38 correlation between \dot{M} and the area was found only for glaciers smaller than 0.1 km² in
39 the Alps, and above 0.1 km², the 1980-2010 mass balances of Swiss glaciers was relatively
490 independent on glacier size [*Fischer et al.*, 2015]. Here we analyzed only glaciers larger
491 than 2 km², which may explain why we did not find such a relationship.

492 The multiple correlations among the predictors complicate the interpretation of the
493 results, but the multivariate linear model can partially separate the contribution of each
494 predictor (Table 2). At first sight, the negative correlation between \dot{M} and the supra-
35 glacial debris cover seems counter intuitive, because debris, when thick enough, is ex-
496 pected to insulate the glacier tongue and reduce ice ablation [e.g., *Østrem*, 1959; *Vin-*
497 *cent et al.*, 2016]. However, this negative correlation is partially induced by the corre-
498 lations between the debris cover and the mean elevation and tongue slope, which are them-
499 selves correlated with \dot{M} (Figure 4). The multivariate linear model shows that the tongue
30 slope and the mean elevation are the best predictors of \dot{M} . These findings can be inter-
501 preted similarly to a modeling study, which found higher mass balance sensitivity to an
502 increase in temperature for debris-covered glaciers, than for debris-free glaciers [*Huss and*
3 *Fischer*, 2016]. The higher sensitivity of debris-covered glaciers and their more negative
504 \dot{M} (compared with debris-free glaciers) could be due to their typical settings at low el-
505 evation and their gentle tongue slope favoring high sensitivity to temperature changes
506 and long response times [*Huss and Fischer*, 2016].

5 Conclusions

We assess the main morphological controls on glacier mass balances of HMA glaciers for the period 2000-2016. The morphological variables have contrasted influences over our twelve studied regions and they explain 8 to 48 % of the mass balance variability. The best predictors of this variability are the slope of the tongue and the mean elevation of the glaciers. The gentler the slope, the more negative the mass balance. Except for Spiti Lahaul and Pamir Alai, the higher the glacier, the less negative or the more positive its mass balance. The influence of the debris cover is less clear than that of the former predictors. In some regions debris-covered glaciers have similar or higher mass balances than debris-free glaciers, and for other regions, we observe the opposite. The influence of the debris is complicated to untangle from the effect of the other morphological variables, because heavily debris-covered tongues are often situated at lower elevation than debris-free tongues, where ablation is higher. Overall, we did not observe systematic differences between debris-free and debris-covered glaciers in terms of glacier mass balances.

Lake-terminating glaciers have more negative mass balances than the region averages. Nevertheless, this effect is not systematic and specific studies need to be conducted on these glaciers to better quantify the lake influence and assess the GLOF hazard.

As the morphological variables explain only a limited fraction of the mass balance variability, we advocate for deeper investigations of the link between climatology, climate change and glacier mass balance. First of all, climatically homogeneous regions have to be defined in an objective way. Once this step is achieved, it would be very interesting to investigate the glacier mass balance sensitivities to temperature and precipitation changes, in order to understand whether the recent mass changes can be attributed to contrasting climate sensitivity or to heterogeneous climate changes. However, this is a great challenge in HMA, since existing large scale climate datasets do not accurately represent conditions at the glacier locations.

533 **Acknowledgments**

534 This work was supported by the French Space Agency (CNES). F.B. and P.W. acknowl-
535 edge funding from the French Service d'Observation GLACIOCLIM and ANR-13-SENV-
536 0005-04/05-PRESHINE. The glacier mass balances data are available through the World
537 Glacier Monitoring Service database (<https://wgms.ch/>) and through the pangaea plat-
538 form (<https://doi.pangaea.de/10.1594/PANGAEA.876545>) for the rate of elevation change
539 maps. The other data are accessible at <http://mountainhydrology.org/data-nature-2017/>
540 and the code used to generate them is available at <https://doi.org/10.5281/zenodo.2548690>.
541 We thank Matthias Huss for insightful discussions and we thank three anonymous re-
542 viewers, the editor in chief and the associate editor who provided comments that greatly
543 improved this manuscript.

544 **References**

- 545 Akaike, H. (1974), A new look at the statistical model identification, *IEEE transac-*
546 *tions on automatic control*, 19(6), 716–723.
- 47 Basnett, S., A. V. Kulkarni, and T. Bolch (2013), The influence of debris cover and
48 glacial lakes on the recession of glaciers in Sikkim Himalaya, India, *Journal of*
549 *Glaciology*, 59, 1035–1046, doi:10.3189/2013JoG12J184.
- 550 Benn, D., T. Bolch, K. Hands, J. Gulley, A. Luckman, L. Nicholson, D. Quincey,
551 S. Thompson, R. Toumi, and S. Wiseman (2012), Response of debris-covered
552 glaciers in the Mount Everest region to recent warming, and implications
553 for outburst flood hazards, *Earth-Science Reviews*, 114(1-2), 156–174, doi:
554 10.1016/j.earscirev.2012.03.008.
- 555 Bernhardt, M., and K. Schulz (2010), SnowSlide: A simple routine for calculat-
556 ing gravitational snow transport, *Geophysical Research Letters*, 37(11), doi:
557 10.1029/2010GL043086.
- 558 Bojinski, S., M. Verstraete, T. C. Peterson, C. Richter, A. Simmons, and M. Zemp
559 (2014), The Concept of Essential Climate Variables in Support of Climate Re-
560 search, Applications, and Policy, *Bulletin of the American Meteorological Society*,
561 95(9), 1431–1443, doi:10.1175/BAMS-D-13-00047.1.
- 562 Brun, F., E. Berthier, P. Wagnon, A. Käab, and D. Treichler (2017), A spatially
563 resolved estimate of High Mountain Asia glacier mass balances from 2000 to 2016,
564 *Nature Geoscience*, 10, 668–673.
- 565 Brun, F., P. Wagnon, E. Berthier, J. M. Shea, W. W. Immerzeel, P. D. A. Kraai-
566 jenbrink, C. Vincent, C. Reverchon, D. Shrestha, and Y. Arnaud (2018), Ice cliff
567 contribution to the tongue-wide ablation of Changri Nup Glacier, Nepal, central
568 Himalaya, *The Cryosphere*, 12(11), 3439–3457, doi:10.5194/tc-12-3439-2018.
- 569 Cogley, J., R. Hock, L. Rasmussen, A. Arendt, A. Bauder, R. Braithwaite, P. Jans-
570 son, G. Kaser, M. Möller, L. Nicholson, et al. (2011), Glossary of glacier mass

- 571 balance and related terms, *IHP-VII technical documents in hydrology*, 86, 965.
- 572 Conrad, O., B. Bechtel, M. Bock, H. Dietrich, E. Fischer, L. Gerlitz, J. Wehberg,
573 V. Wichmann, and J. Böhner (2015), System for Automated Geoscientific Anal-
574 yses (SAGA) v. 2.1.4, *Geoscientific Model Development*, 8(7), 1991–2007, doi:
575 10.5194/gmd-8-1991-2015.
- 576 Cuffey, K. M., and W. S. B. Paterson (2010), *The physics of glaciers*, Academic
577 Press.
- 578 Dehecq, A., N. Gourmelen, A. S. Gardner, F. Brun, D. Goldberg, P. W. Nienow,
579 E. Berthier, C. Vincent, P. Wagnon, and E. Trouv (2019), Twenty-first century
580 glacier slowdown driven by mass loss in High Mountain Asia, *Nature Geoscience*,
581 12(1), 22–27, doi:10.1038/s41561-018-0271-9.
- 582 Farr, T. G., P. A. Rosen, E. Caro, R. Crippen, R. Duren, S. Hensley, M. Kobrick,
583 M. Paller, E. Rodriguez, L. Roth, D. Seal, S. Shaffer, J. Shimada, J. Umland,
584 M. Werner, M. Oskin, D. Burbank, and D. Alsdorf (2007), The Shuttle Radar
585 Topography Mission, *Reviews of Geophysics*, 45(2), doi:10.1029/2005RG000183.
- 586 Fischer, M., M. Huss, and M. Hoelzle (2015), Surface elevation and mass changes of
587 all Swiss glaciers 1980–2010, *The Cryosphere*, 9(2), 525–540, doi:10.5194/tc-9-525-
588 2015.
- 589 Forsythe, N., H. J. Fowler, X.-F. Li, S. Blenkinsop, and D. Pritchard (2017),
590 Karakoram temperature and glacial melt driven by regional atmospheric circu-
591 lation variability, *Nature Climate Change*, 7, 664–670, doi:10.1038/nclimate3361.
- 592 Freeman, T. G. (1991), Calculating catchment area with divergent flow
593 based on a regular grid, *Computers & Geosciences*, 17(3), 413 – 422, doi:
594 [https://doi.org/10.1016/0098-3004\(91\)90048-I](https://doi.org/10.1016/0098-3004(91)90048-I).
- 595 Gardelle, J., E. Berthier, and Y. Arnaud (2012), Impact of resolution and radar pen-
596 etration on glacier elevation changes computed from DEM differencing, *Journal of*
597 *Glaciology*, 58(208), 419–422, doi:doi:10.3189/2012JoG11J175.

- 598 Gardelle, J., E. Berthier, Y. Arnaud, and A. Kääb (2013), Region-wide glacier mass
599 balances over the Pamir-Karakoram-Himalaya during 1999-2011, *The Cryosphere*,
600 7(4), 1263–1286, doi:10.5194/tc-7-1263-2013.
- 601 Gardner, A. S., G. Moholdt, J. G. Cogley, B. Wouters, A. A. Arendt, J. Wahr,
602 E. Berthier, R. Hock, W. T. Pfeffer, G. Kaser, S. R. M. Ligtenberg, T. Bolch,
603 M. J. Sharp, J. O. Hagen, M. R. van den Broeke, and F. Paul (2013), A Recon-
604 ciled Estimate of Glacier Contributions to Sea Level Rise: 2003 to 2009, *Science*,
605 340, 852–857, doi:10.1126/science.1234532.
- 606 Haritashya, U. K., J. S. Kargel, D. H. Shugar, G. J. Leonard, K. Strattman, C. S.
607 Watson, D. Shean, S. Harrison, K. T. Mandli, and D. Regmi (2018), Evolution
608 and Controls of Large Glacial Lakes in the Nepal Himalaya, *Remote Sensing*,
609 10(5), doi:10.3390/rs10050798.
- 610 Herreid, S., and F. Pellicciotti (2018), Automated detection of ice cliffs within
611 supraglacial debris cover, *The Cryosphere*, 12(5), 1811–1829, doi:10.5194/tc-
612 12-1811-2018.
- 613 Hocking, R. R. (1976), The Analysis and Selection of Variables in Linear Regression,
614 *Biometrics*, 32(1), 1–49, doi:10.2307/2529336.
- 615 Huss, M. (2012), Extrapolating glacier mass balance to the mountain-range scale:
616 the European Alps 1900-2010, *The Cryosphere*, 6(4), 713–727, doi:10.5194/tc-6-
617 713-2012.
- 618 Huss, M., and M. Fischer (2016), Sensitivity of Very Small Glaciers in the
619 Swiss Alps to Future Climate Change, *Frontiers in Earth Science*, 4, 34, doi:
620 10.3389/feart.2016.00034.
- 621 Huss, M., R. Hock, A. Bauder, and M. Funk (2012), Conventional versus
622 reference-surface mass balance, *Journal of Glaciology*, 58(208), 278–286, doi:
623 10.3189/2012JoG11J216.
- 624 Janke, J. R., A. C. Bellisario, and F. A. Ferrando (2015), Classification of debris-
625 covered glaciers and rock glaciers in the Andes of central Chile, *Geomorphology*,

626 241, 98–121, doi:10.1016/j.geomorph.2015.03.034.

627 Jomelli, V., I. Pavlova, N. Eckert, D. Grancher, and D. Brunstein (2015), A
628 new hierarchical Bayesian approach to analyse environmental and climatic
629 influences on debris flow occurrence, *Geomorphology*, *250*, 407–421, doi:
630 10.1016/j.geomorph.2015.05.022.

631 Kääb, A., E. Berthier, C. Nuth, J. Gardelle, and Y. Arnaud (2012), Contrasting pat-
632 terns of early twenty-first-century glacier mass change in the Himalayas, *Nature*,
633 *488*(7412), 495–498, doi:10.1038/nature11324.

634 Kääb, A., D. Treichler, C. Nuth, and E. Berthier (2015), Brief Communication:
635 Contending estimates of 2003–2008 glacier mass balance over the PamirKarako-
636 ramHimalaya, *The Cryosphere*, *9*(2), 557–564, doi:10.5194/tc-9-557-2015.

637 Kapnick, S. B., T. L. Delworth, M. Ashfaq, S. Malyshev, and P. C. D. Milly (2014),
638 Snowfall less sensitive to warming in Karakoram than in Himalayas due to a
639 unique seasonal cycle, *Nature Geoscience*, *7*, 834–840, doi:10.1038/ngeo2269.

640 Khanal, N. R., P. K. Mool, A. B. Shrestha, G. Rasul, P. K. Ghimire, R. B. Shrestha,
641 and S. P. Joshi (2015), A comprehensive approach and methods for glacial lake
642 outburst flood risk assessment, with examples from Nepal and the transboundary
643 area, *International Journal of Water Resources Development*, *31*(2), 219–237,
644 doi:10.1080/07900627.2014.994116.

645 King, O., D. J. Quincey, J. L. Carrivick, and A. V. Rowan (2017), Spatial variability
646 in mass loss of glaciers in the Everest region, central Himalayas, between 2000 and
647 2015, *The Cryosphere*, *11*(1), 407–426, doi:10.5194/tc-11-407-2017.

648 King, O., A. Dehecq, D. Quincey, and J. Carrivick (2018), Contrasting ge-
649 ometric and dynamic evolution of lake and land-terminating glaciers in
650 the central Himalaya, *Global and Planetary Change*, *167*, 46–60, doi:
651 10.1016/j.gloplacha.2018.05.006.

652 Kraaijenbrink, P. D. A., M. F. P. Bierkens, A. F. Lutz, and W. W. Immerzeel
653 (2017), Impact of a global temperature rise of 1.5 degrees Celsius on Asia glaciers,

654 *Nature*, 549, 257–260, doi:10.1038/nature23878.

655 Maharjan, S. B., P. K. Mool, W. Lizong, G. Xiao, F. Shrestha, R. Shrestha,
656 N. Khanal, S. R. Bajracharya, S. Joshi, S. Shai, and P. Baral (2018), The status of
657 glacial lakes in the Hindu Kush Himalaya, *Tech. rep.*, ICIMOD, Kathmandu.

658 Maussion, F., D. Scherer, T. Mlg, E. Collier, J. Curio, and R. Finkelburg (2014),
659 Precipitation Seasonality and Variability over the Tibetan Plateau as Re-
660 solved by the High Asia Reanalysis, *Journal of Climate*, 27(5), 1910–1927, doi:
661 10.1175/JCLI-D-13-00282.1.

662 Nicholson, L., and D. I. Benn (2006), Calculating ice melt beneath a debris
663 layer using meteorological data, *Journal of Glaciology*, 52, 463–470, doi:
664 10.3189/172756506781828584.

665 Nuimura, T., K. Fujita, S. Yamaguchi, and R. R. Sharma (2012), Elevation changes
666 of glaciers revealed by multitemporal digital elevation models calibrated by GPS
667 survey in the Khumbu region, Nepal Himalaya, 1992-2008, *Journal of Glaciology*,
668 58(210), 648–656, doi:10.3189/2012JoG11J061.

669 Oerlemans, J., and B. K. Reichert (2000), Relating glacier mass balance to meteo-
670 rological data by using a seasonal sensitivity characteristic, *Journal of Glaciology*,
671 46(152), 1–6, doi:10.3189/172756500781833269.

672 Østrem, G. (1959), Ice Melting under a Thin Layer of Moraine, and the Existence of
673 Ice Cores in Moraine Ridges, *Geografiska Annaler*, 41(4), pp. 228–230.

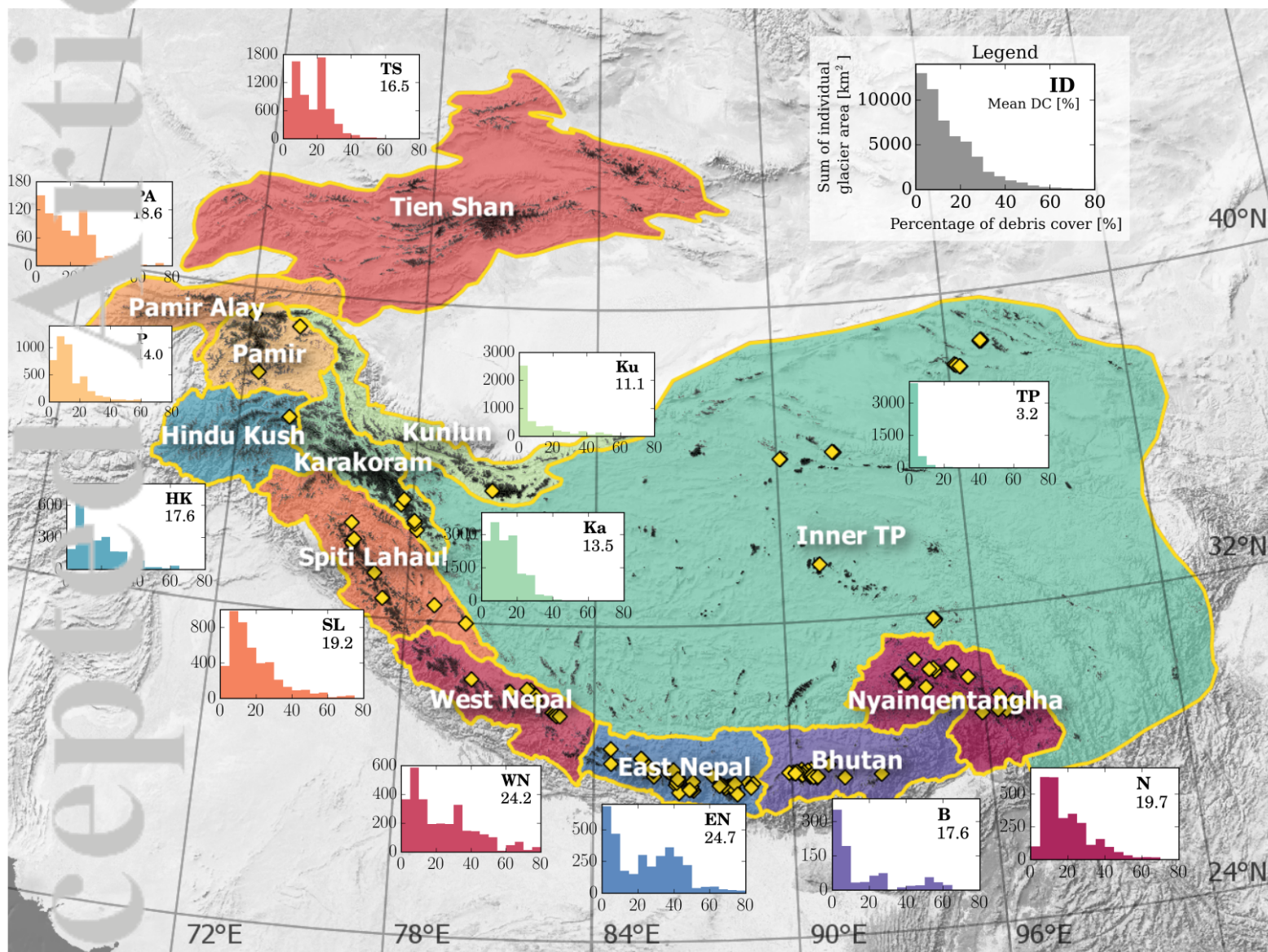
674 Paul, F., and W. Haeberli (2008), Spatial variability of glacier elevation changes in
675 the Swiss Alps obtained from two digital elevation models, *Geophysical Research*
676 *Letters*, 35(21), doi:10.1029/2008GL034718.

677 Paul, F., N. E. Barrand, S. Baumann, E. Berthier, T. Bolch, K. Casey, H. Frey,
678 S. P. Joshi, V. Konovalov, R. Le Bris, N. Mölg, G. Nosenko, C. Nuth, A. Pope,
679 A. Racoviteanu, P. Rastner, B. Raup, K. Scharer, S. Steffen, and S. Winsvold
680 (2013), On the accuracy of glacier outlines derived from remote-sensing data,
681 *Annals of Glaciology*, 54, 171–182, doi:10.3189/2013AoG63A296.

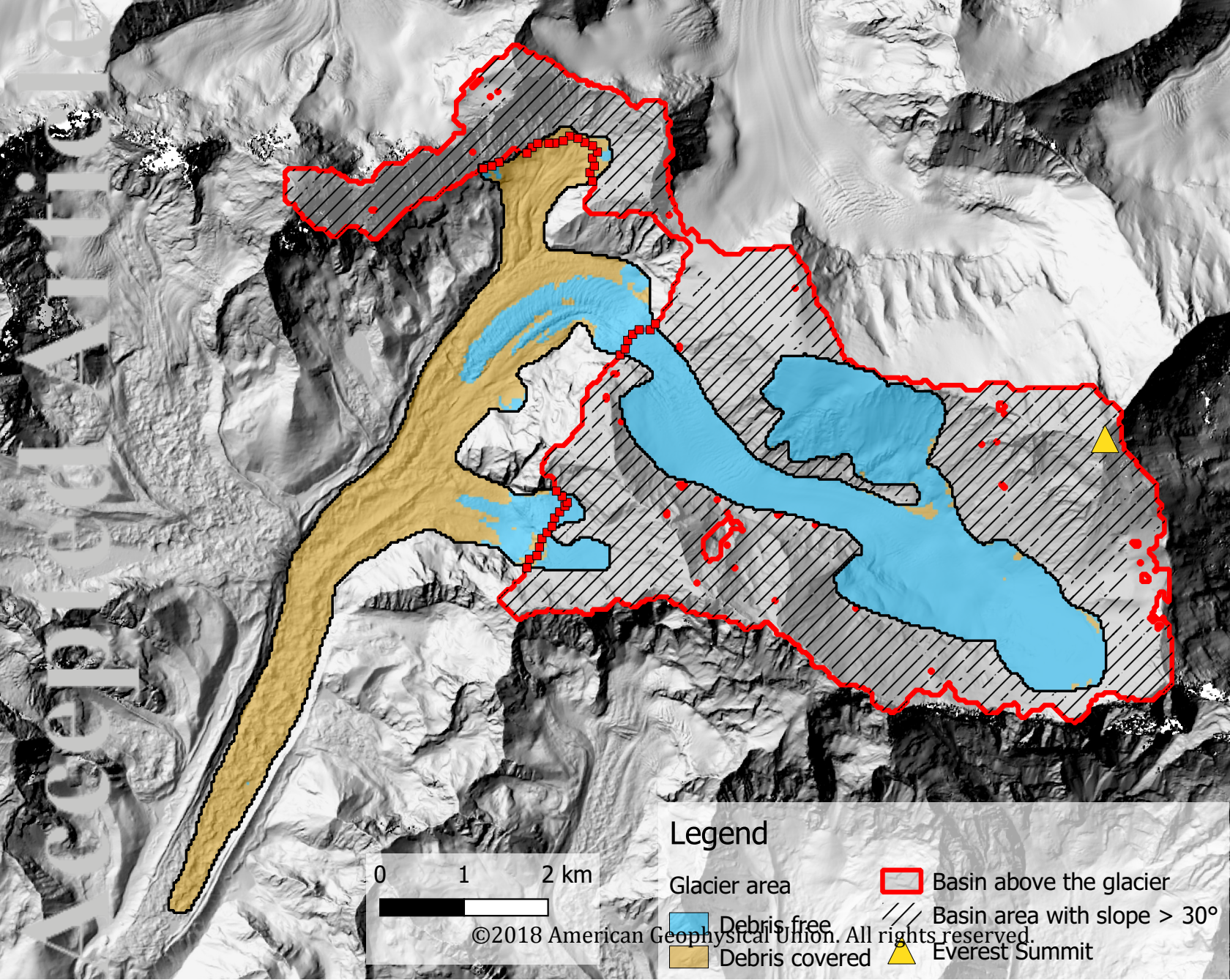
- 682 Pfeffer, W. T., A. A. Arendt, A. Bliss, T. Bolch, J. G. Cogley, A. S. Gardner, J.-
683 O. Hagen, R. Hock, G. Kaser, C. Kienholz, E. S. Miles, G. Moholdt, N. Mölg,
684 F. Paul, V. Radic, P. Rastner, B. H. Raup, J. Rich, and M. J. Sharp (2014), The
685 Randolph Glacier Inventory: a globally complete inventory of glaciers, *Journal of*
686 *Glaciology*, *60*, 537–552, doi:10.3189/2014JoG13J176.
- 687 Quincey, D. J., S. D. Richardson, A. Luckman, R. M. Lucas, J. M. Reynolds, M. J.
688 Hambrey, and N. F. Glasser (2007), Early recognition of glacial lake hazards in
689 the Himalaya using remote sensing datasets, *Global and Planetary Change*, *56*,
690 137–152, doi:10.1016/j.gloplacha.2006.07.013.
- 691 Rabatel, A., A. Letréguilly, J.-P. Dedieu, and N. Eckert (2013), Changes in glacier
692 equilibrium-line altitude in the western Alps from 1984 to 2010: evaluation by
693 remote sensing and modeling of the morpho-topographic and climate controls, *The*
694 *Cryosphere*, *7*(5), 1455–1471, doi:10.5194/tc-7-1455-2013.
- 695 Rabatel, A., J. P. Dedieu, and C. Vincent (2016), Spatio-temporal changes in
696 glacier-wide mass balance quantified by optical remote sensing on 30 glaciers in
697 the French Alps for the period 1983-2014, *Journal of Glaciology*, *62*(236), 1153–
698 1166, doi:10.1017/jog.2016.113.
- 699 Röhl, K. (2006), Thermo-erosional notch development at fresh-water-calving
700 Tasman Glacier, New Zealand, *Journal of Glaciology*, *52*(177), 203–213, doi:
701 10.3189/172756506781828773.
- 702 Rolstad, C., T. Haug, and B. Denby (2009), Spatially integrated geodetic glacier
703 mass balance and its uncertainty based on geostatistical analysis: application to
704 the western Svartisen ice cap, Norway, *Journal of Glaciology*, *55*(192), 666–680,
705 doi:10.3189/002214309789470950.
- 706 Rowan, A. V. (2017), The 'Little Ice Age' in the Himalaya: A review of glacier ad-
707 vance driven by Northern Hemisphere temperature change, *The Holocene*, *27*,
708 292–308, doi:10.1177/0959683616658530.

- 709 Rowan, A. V., D. L. Egholm, D. J. Quincey, and N. F. Glasser (2015), Modelling
710 the feedbacks between mass balance, ice flow and debris transport to predict the
711 response to climate change of debris-covered glaciers in the Himalaya, *Earth and*
712 *Planetary Science Letters*, *430*, 427–438, doi:10.1016/j.epsl.2015.09.004.
- 713 Sakai, A., and K. Fujita (2017), Contrasting glacier responses to recent cli-
714 mate change in high-mountain Asia, *Scientific Reports*, *7*(1), 13,717, doi:
715 10.1038/s41598-017-14256-5.
- 716 Salerno, F., S. Thakuri, G. Tartari, T. Nuimura, S. Sunako, A. Sakai, and K. Fu-
717 jita (2017), Debris-covered glacier anomaly? Morphological factors controlling
718 changes in the mass balance, surface area, terminus position, and snow line al-
719 titude of Himalayan glaciers, *Earth and Planetary Science Letters*, *471*, 19 – 31,
720 doi:https://doi.org/10.1016/j.epsl.2017.04.039.
- 721 Scherler, D., B. Bookhagen, and M. R. Strecker (2011a), Hillslope-glacier coupling:
722 The interplay of topography and glacial dynamics in High Asia, *Journal of Geo-*
723 *physical Research: Earth Surface*, *116*(F2), doi:10.1029/2010JF001751.
- 724 Scherler, D., B. Bookhagen, and M. R. Strecker (2011b), Spatially variable response
725 of Himalayan glaciers to climate change affected by debris cover, *Nature Geo-*
726 *science*, *4*, 156–159, doi:10.1038/ngeo1068.
- 727 Shean, D. (2017), *High Mountain Asia 8-meter DEM Mosaics Derived from Optical*
728 *Imagery, Version 1*, Boulder, Colorado USA. NASA National Snow and Ice Data
729 Center Distributed Active Archive Center, doi:10.5067/KXOVQ9L172S2 [Accessed
730 in March 2019].
- 731 Thompson, S. S., D. I. Benn, K. Dennis, and A. Luckman (2012), A rapidly growing
732 moraine-dammed glacial lake on Ngozumpa Glacier, Nepal, *Geomorphology*, *145*,
733 1–11, doi:10.1016/j.geomorph.2011.08.015.
- 734 Tribe, A. (1992), Automated recognition of valley lines and drainage networks from
735 grid digital elevation models: a review and a new method, *Journal of Hydrology*,
736 *139*(1), 263–293, doi:10.1016/0022-1694(92)90206-B.

- 737 Vincent, C., P. Wagnon, J. M. Shea, W. W. Immerzeel, P. Kraaijenbrink,
738 D. Shrestha, A. Soruco, Y. Arnaud, F. Brun, E. Berthier, and S. F. Sherpa (2016),
739 Reduced melt on debris-covered glaciers: investigations from Changri Nup Glacier,
740 Nepal, *The Cryosphere*, *10*(4), 1845–1858, doi:10.5194/tc-10-1845-2016.
- 741 Vincent, C., A. Fischer, C. Mayer, A. Bauder, S. P. Galos, M. Funk, E. Thibert,
742 D. Six, L. Braun, and M. Huss (2017), Common climatic signal from glaciers in
743 the European Alps over the last 50 years, *Geophysical Research Letters*, *44*, 1376–
744 1383, doi:10.1002/2016GL072094.
- 745 Wirbel, A., A. H. Jarosch, and L. Nicholson (2018), Modelling debris transport
746 within glaciers by advection in a full-Stokes ice flow model, *The Cryosphere*,
747 *12*(1), 189–204, doi:10.5194/tc-12-189-2018.
- 748 Xiang, Y., T. Yao, Y. Gao, G. Zhang, W. Wang, and L. Tian (2018), Retreat rates
749 of debris-covered and debris-free glaciers in the Koshi River Basin, central Hi-
750 malayas, from 1975 to 2010, *Environmental Earth Sciences*, *77*(7), 285.
- 751 Zhang, G., T. Yao, C. K. Shum, S. Yi, K. Yang, H. Xie, W. Feng, T. Bolch,
752 L. Wang, A. Behrangi, H. Zhang, W. Wang, Y. Xiang, and J. Yu (2017), Lake
753 volume and groundwater storage variations in Tibetan Plateau’s endorheic basin,
754 *Geophysical Research Letters*, *44*(11), 5550–5560, doi:10.1002/2017GL073773.



2018JF004838-f01-z-.png



Legend

Glacier area

Debris free

Debris covered

Basin above the glacier

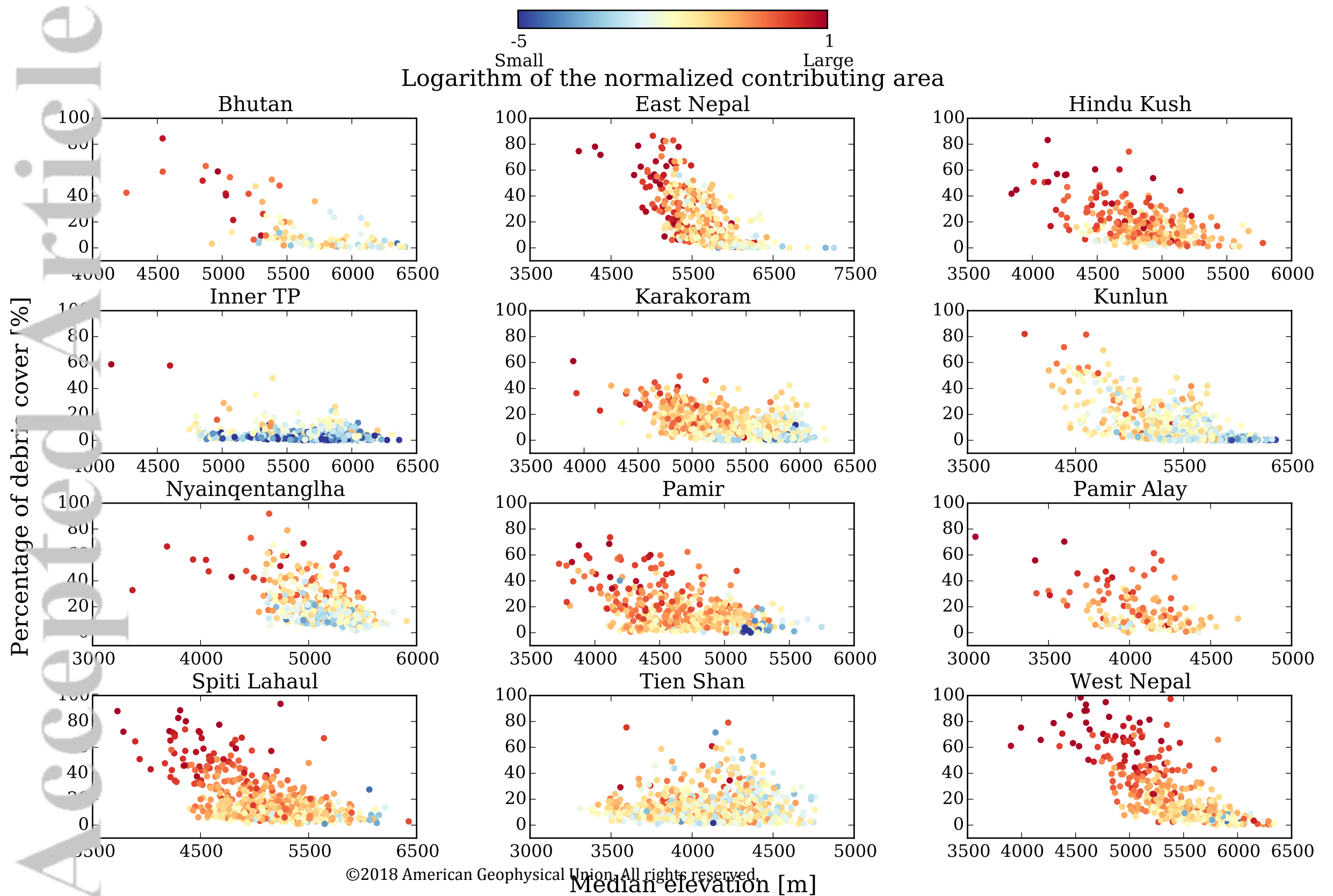
Basin area with slope > 30°

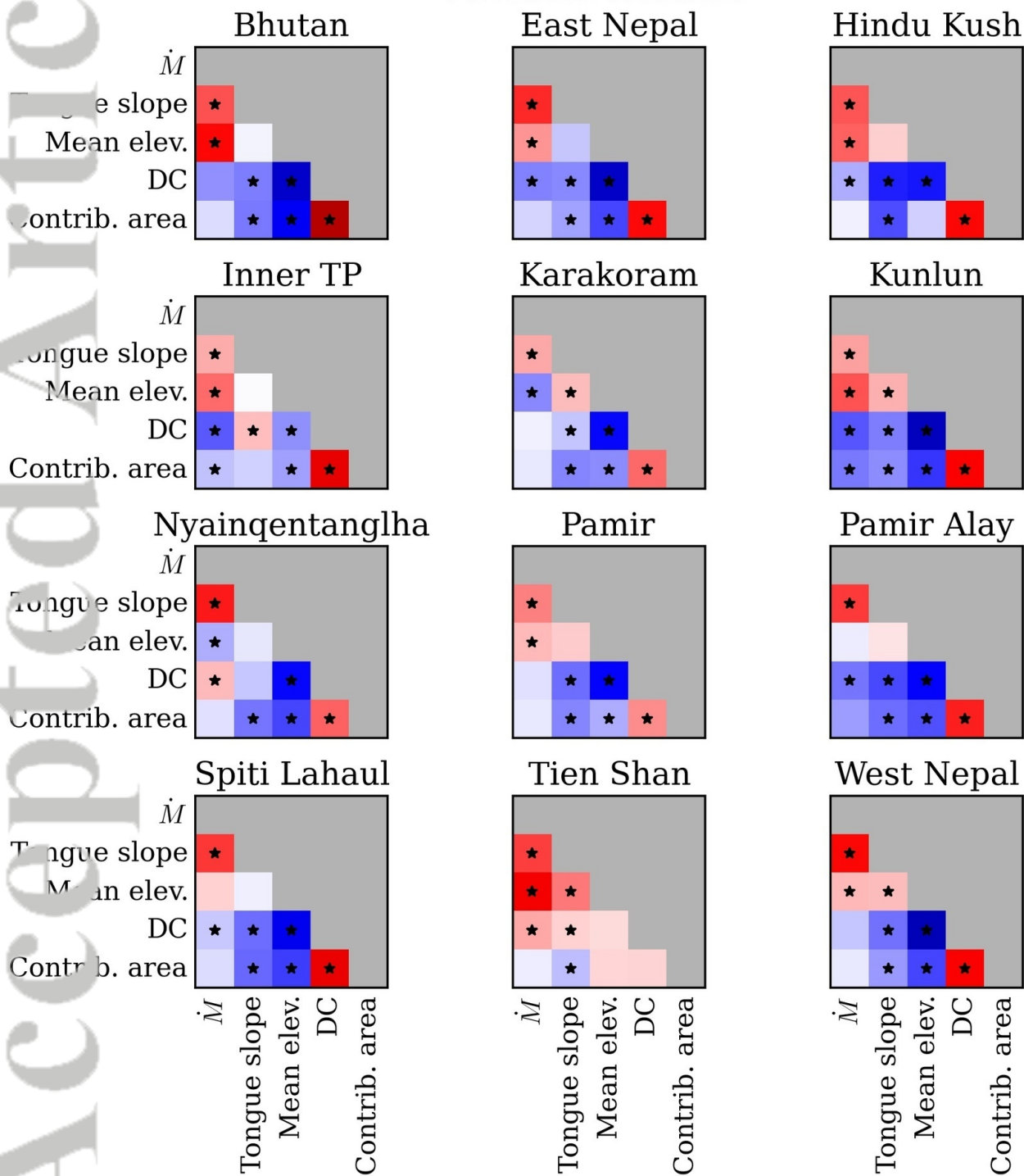
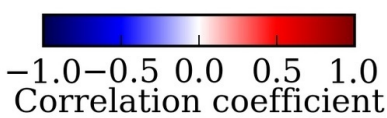
Everest Summit

0 1 2 km



©2018 American Geophysical Union. All rights reserved.





2018JF004838-f04-z-.jpg

Area weighted
mass balance
[m w.e. yr⁻¹]

▲ debris-free glaciers ● debris-covered glaciers

